thesis2024

Joana Belmiro

2024-12-25

Table of contents

Acknowledgments

This is a Quarto book.

To learn more about Quarto books visit <https://quarto.org/docs/books>.

```r
1 + 1
```

```
[1] 2
```

1 Abstract

In summary, this book has no content whatsoever.

```
1 + 1
```

```
[1] 2
```

2 Introduction

This is a book created from markdown and executable code.

See Knuth (1984) for additional discussion of literate programming.

```
1 + 1
```

```
[1] 2
```

3 Creating frames of reference for chert exploitation during the Late Pleistocene in Southwesternmost Iberia

4 Within and Beyond: Chert Procurement Patterns During The Upper Palaeolithic in Southwesternmost Iberia

5 geochemistry

5.1 X-ray diffraction (XRD)

Some text. Some other text. A bit more of text.

5.2 Scanning electron microscopy and energy dispersive X-ray spectroscopy (SEM-EDS)

5.3 Portable X-ray fluorescence (pXRF)

```
Call:

PCA(X = df_scaled_alg, graph = FALSE)




Eigenvalues
```

	Dim.1	Dim.2	Dim.3	Dim.4	Dim.5	Dim.6	Dim.7
Variance	2.419	1.842	1.009	0.800	0.663	0.151	0.116
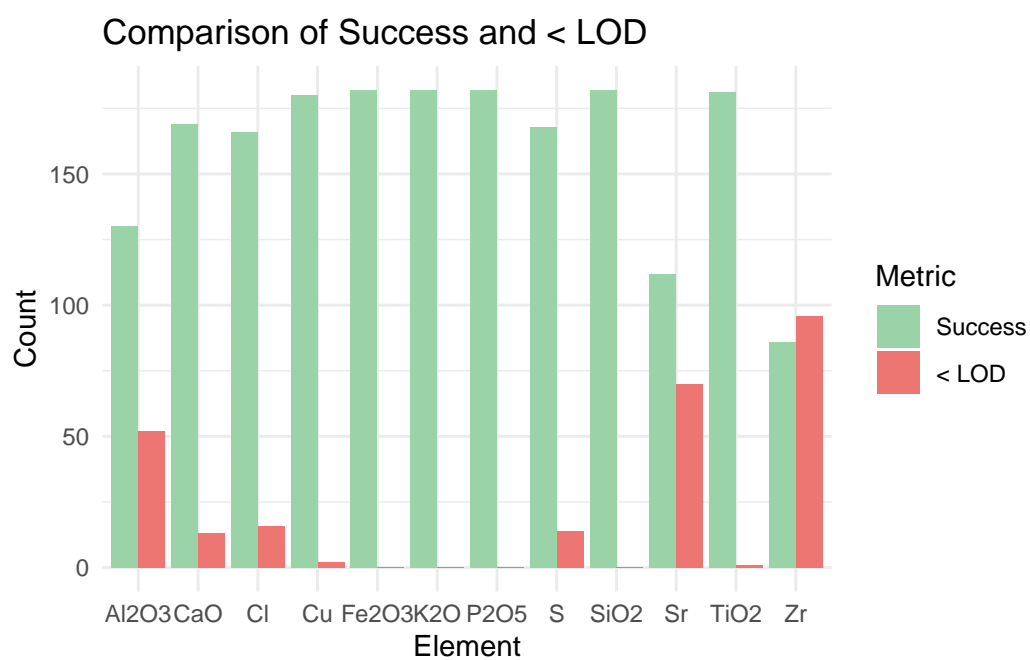
Figure 5.1: A barplot.
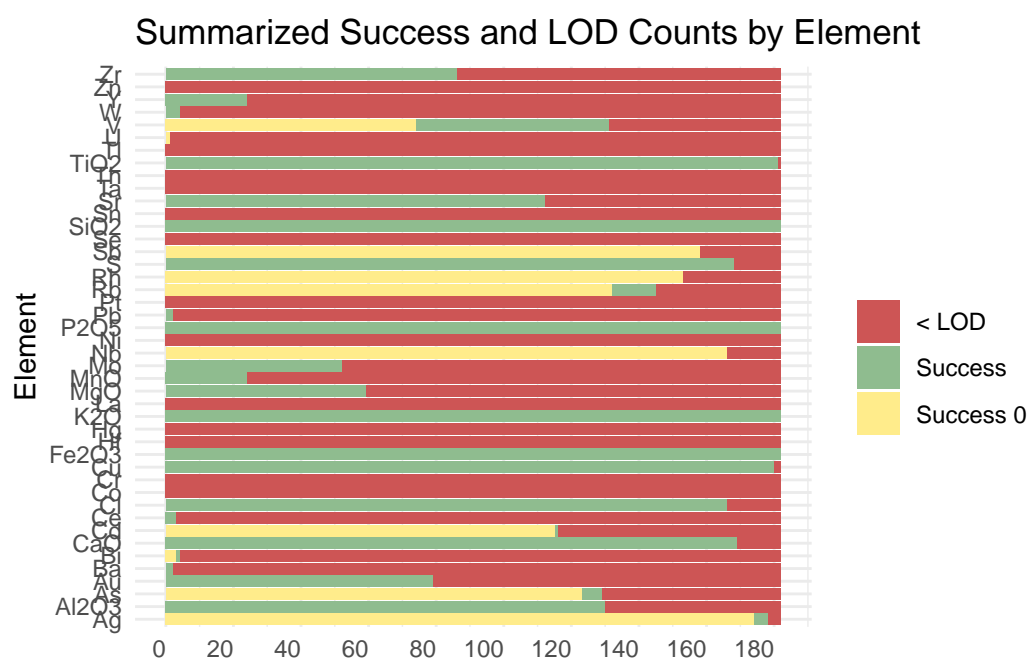
Figure 5.2: A barplot.

```
% of var.               34.558  26.319  14.408  11.424   9.477   2.154   1.660

Cumulative % of var.  34.558  60.877  75.284  86.708  96.186  98.340 100.000
```

Individuals (the 10 first)

```
          Dist    Dim.1   ctr   cos2    Dim.2   ctr   cos2    Dim.3   ctr
LJW   |  5.517 |  2.737  4.995  0.246 | -1.311  1.504  0.056 |  2.627 11.035
LJW.1 |  3.781 |  3.129  6.527  0.685 | -1.509  1.995  0.159 | -0.957  1.465
LJW.2 |  5.036 |  2.464  4.047  0.239 |  2.696  6.365  0.287 |  2.566 10.531
LJW.3 |  1.616 |  0.869  0.503  0.289 | -1.289  1.455  0.636 | -0.092  0.013
LJW.4 |  6.734 |  3.205  6.849  0.227 |  4.295 16.149  0.407 |  3.622 20.978
LJW.5 |  3.092 | -2.104  2.952  0.463 |  2.084  3.804  0.455 | -0.332  0.176
LJW.6 |  2.173 |  1.088  0.789  0.251 | -1.751  2.683  0.649 | -0.387  0.240
LJW.7 |  1.942 |  1.247  1.036  0.412 | -1.282  1.440  0.436 | -0.305  0.148
LJW.8 |  3.021 |  2.064  2.840  0.467 | -1.639  2.352  0.294 | -0.995  1.582
LJW.9 |  6.299 |  4.211 11.824  0.447 |  3.056  8.174  0.235 | -1.359  2.953
         cos2
LJW    0.227 |
LJW.1  0.064 |
LJW.2  0.260 |
LJW.3  0.003 |
LJW.4  0.289 |
LJW.5  0.012 |
LJW.6  0.032 |
```

```
LJW.7  0.025 |

LJW.8  0.108 |

LJW.9  0.047 |


Variables

          Dim.1    ctr   cos2    Dim.2    ctr   cos2    Dim.3    ctr   cos2

P2O5  |  0.805 26.793  0.648 |  0.490 13.038  0.240 | -0.148  2.184  0.022 |

S     |  0.659 17.966  0.435 |  0.491 13.067  0.241 | -0.154  2.358  0.024 |

Cl    |  0.360  5.358  0.130 |  0.474 12.190  0.225 |  0.611 37.034  0.374 |

K2O   |  0.667 18.400  0.445 | -0.675 24.757  0.456 | -0.141  1.971  0.020 |

CaO   |  0.081  0.270  0.007 |  0.596 19.287  0.355 | -0.379 14.249  0.144 |

TiO2  |  0.730 22.056  0.534 | -0.530 15.270  0.281 | -0.223  4.925  0.050 |

Fe2O3 |  0.471  9.157  0.222 | -0.210  2.391  0.044 |  0.613 37.279  0.376 |
```

Scree plot
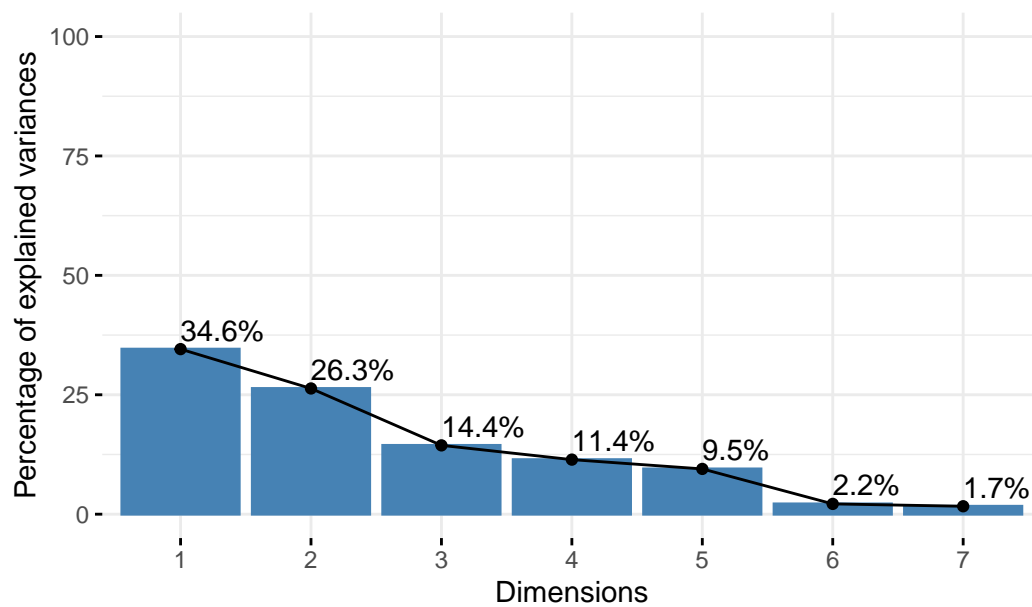
```
Call:

PCA(X = df_scaled_nl, graph = FALSE)


Eigenvalues

                        Dim.1   Dim.2   Dim.3   Dim.4   Dim.5   Dim.6

Variance                2.933   1.713   0.672   0.354   0.249   0.079

% of var.              48.885  28.546  11.197   5.901   4.157   1.314

Cumulative % of var.   48.885  77.431  88.628  94.529  98.686 100.000


Individuals (the 10 first)

          Dist    Dim.1   ctr   cos2    Dim.2   ctr   cos2    Dim.3   ctr

CPT   | 1.744 | -1.714  1.411  0.967 | -0.066  0.004  0.001 | -0.142  0.042

CPT.1 | 1.797 | -1.356  0.884  0.570 |  0.402  0.133  0.050 |  1.046  2.295

CPT.2 | 1.426 | -1.330  0.850  0.870 | -0.353  0.103  0.061 | -0.060  0.008

CPT.3 | 1.825 | -1.803  1.561  0.975 | -0.070  0.004  0.001 | -0.084  0.015

CPT.4 | 1.815 | -1.703  1.393  0.881 | -0.332  0.090  0.033 | -0.360  0.272

CPT.5 | 1.224 | -0.702  0.237  0.329 | -0.651  0.348  0.282 | -0.659  0.911

CPT.6 | 1.542 | -1.503  1.085  0.951 | -0.100  0.008  0.004 | -0.197  0.081

CPT.7 | 1.883 | -1.787  1.534  0.901 | -0.216  0.038  0.013 | -0.432  0.391

CPT.8 | 1.592 | -1.544  1.145  0.941 |  0.056  0.003  0.001 |  0.099  0.020

CPT.9 | 1.712 | -1.523  1.114  0.792 |  0.441  0.160  0.066 |  0.475  0.474
```

```
         cos2

CPT    0.007 |

CPT.1  0.339 |

CPT.2  0.002 |

CPT.3  0.002 |

CPT.4  0.039 |

CPT.5  0.290 |

CPT.6  0.016 |

CPT.7  0.053 |

CPT.8  0.004 |

CPT.9  0.077 |
```

Variables

	Dim.1	ctr	cos2	Dim.2	ctr	cos2	Dim.3	ctr	cos2
P2O5	0.668	15.194	0.446	0.591	20.375	0.349	-0.119	2.094	0.014
K2O	0.836	23.802	0.698	-0.463	12.504	0.214	-0.073	0.791	0.005
TiO2	0.886	26.789	0.786	-0.370	7.986	0.137	-0.053	0.411	0.003
Fe2O3	0.844	24.304	0.713	-0.237	3.278	0.056	0.110	1.797	0.012
Cu	0.411	5.761	0.169	0.632	23.299	0.399	0.637	60.406	0.406
S	0.349	4.150	0.122	0.747	32.557	0.558	-0.481	34.501	0.232

Scree plot
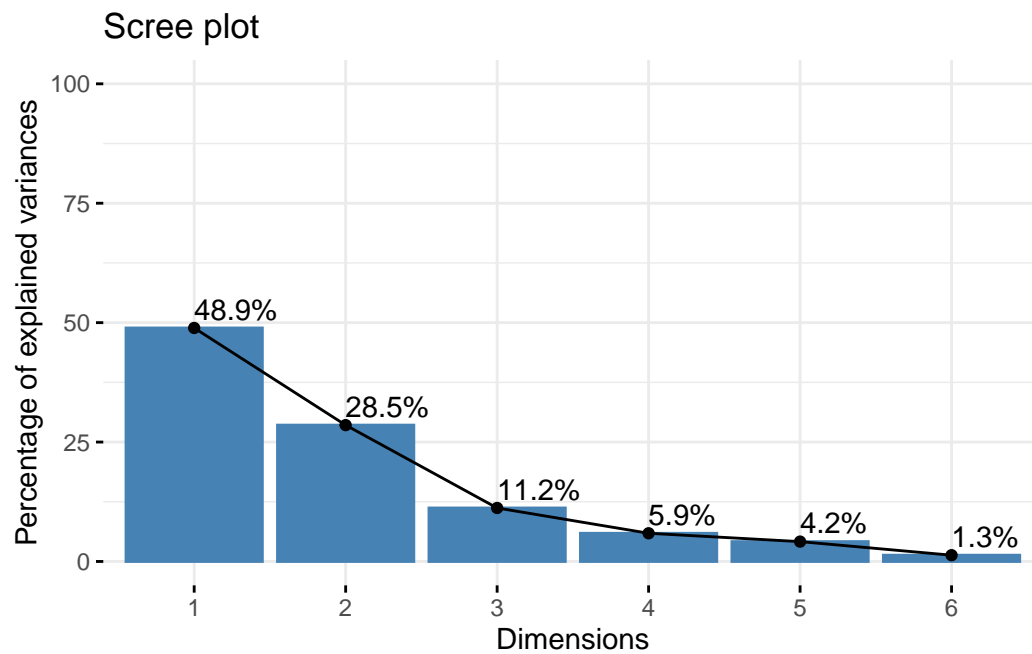

```
Call:

PCA(X = df_scaled_comp, graph = FALSE)
```

Eigenvalues

	Dim.1	Dim.2	Dim.3	Dim.4	Dim.5	Dim.6
Variance	2.729	1.753	0.712	0.456	0.247	0.103
% of var.	45.477	29.222	11.871	7.600	4.121	1.709
Cumulative % of var.	45.477	74.699	86.570	94.170	98.291	100.000

Individuals (the 10 first)

|	Dist	Dim.1	ctr	cos2	Dim.2	ctr	cos2	Dim.3	ctr

```
CPT   |  1.872 | -1.795  1.639  0.919 |  0.369  0.108  0.039 | -0.111  0.024
CPT.1 |  1.907 | -1.389  0.982  0.531 |  0.687  0.374  0.130 |  0.936  1.710
CPT.2 |  1.356 | -1.275  0.827  0.884 | -0.107  0.009  0.006 |  0.041  0.003
CPT.3 |  2.000 | -1.935  1.907  0.936 |  0.426  0.144  0.045 | -0.116  0.026
CPT.4 |  1.850 | -1.773  1.600  0.918 |  0.089  0.006  0.002 | -0.328  0.209
CPT.5 |  1.308 | -0.359  0.066  0.075 | -0.852  0.574  0.424 | -0.776  1.174
CPT.6 |  1.570 | -1.502  1.149  0.915 |  0.237  0.045  0.023 | -0.150  0.044
CPT.7 |  1.991 | -1.882  1.802  0.894 |  0.248  0.049  0.016 | -0.399  0.310
CPT.8 |  1.674 | -1.552  1.225  0.860 |  0.353  0.099  0.044 |  0.044  0.004
CPT.9 |  1.986 | -1.618  1.333  0.664 |  0.979  0.759  0.243 |  0.475  0.440
        cos2
CPT    0.003 |
CPT.1  0.241 |
CPT.2  0.001 |
CPT.3  0.003 |
CPT.4  0.031 |
CPT.5  0.352 |
CPT.6  0.009 |
CPT.7  0.040 |
CPT.8  0.001 |
CPT.9  0.057 |
```

Variables

```
         Dim.1    ctr   cos2    Dim.2    ctr   cos2    Dim.3    ctr   cos2

P2O5  |  0.663 16.108  0.440 |  0.620 21.955  0.385 | -0.190  5.080  0.036 |

K2O   |  0.712 18.598  0.507 | -0.630 22.626  0.397 | -0.108  1.653  0.012 |

TiO2  |  0.800 23.482  0.641 | -0.491 13.763  0.241 | -0.048  0.321  0.002 |

Fe2O3 |  0.751 20.672  0.564 | -0.247  3.491  0.061 |  0.295 12.221  0.087 |

Cu    |  0.463  7.866  0.215 |  0.576 18.943  0.332 |  0.617 53.383  0.380 |

S     |  0.602 13.273  0.362 |  0.581 19.222  0.337 | -0.441 27.342  0.195 |
```


Scree plot
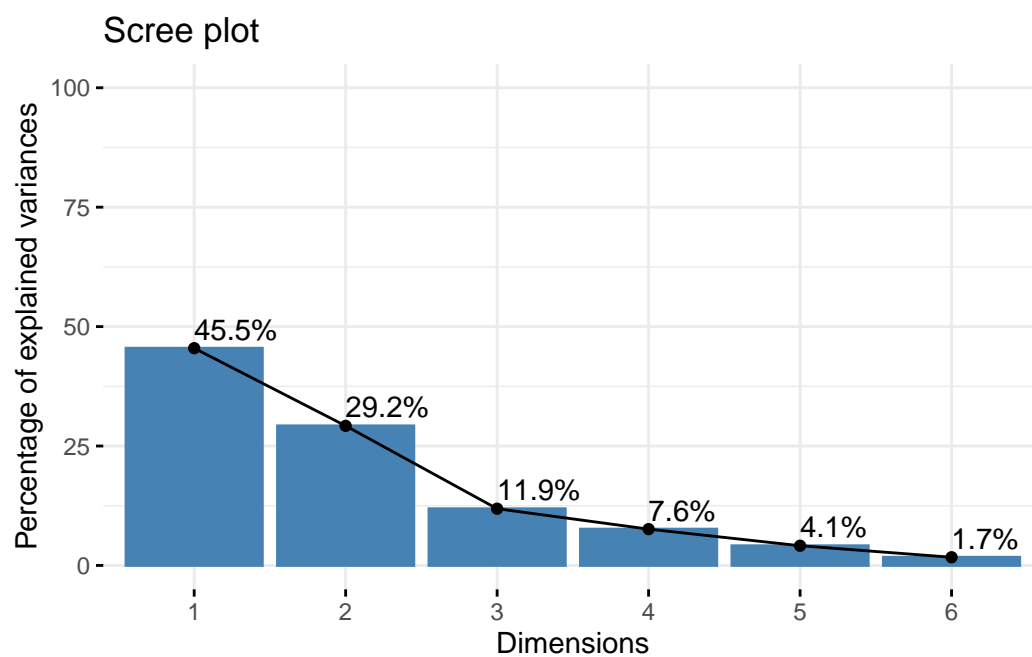
Call:

PCA(X = df_scaled_comp2, graph = FALSE)

Eigenvalues

16

	Dim.1	Dim.2	Dim.3	Dim.4	Dim.5	Dim.6
Variance	3.074	1.638	0.687	0.329	0.237	0.035
% of var.	51.229	27.306	11.444	5.478	3.956	0.588
Cumulative % of var.	51.229	78.534	89.978	95.456	99.412	100.000

Individuals (the 10 first)

	Dist		Dim.1	ctr	cos2	Dim.2	ctr	cos2	Dim.3	ctr
LJW	3.502	|	1.688	0.997	0.232	-0.419	0.115	0.014	0.306	0.147
LJW.1	1.452	|	1.128	0.445	0.604	0.594	0.232	0.168	-0.644	0.649
LJW.2	2.521	|	0.866	0.262	0.118	1.892	2.350	0.563	-1.389	3.020
LJW.3	0.560	|	0.044	0.001	0.006	-0.390	0.100	0.485	-0.313	0.153
LJW.4	3.148	|	1.069	0.400	0.115	2.767	5.026	0.773	-0.431	0.290
LJW.5	1.545	|	-1.026	0.368	0.441	0.339	0.076	0.048	-1.094	1.876
LJW.6	0.899	|	0.196	0.013	0.048	-0.082	0.004	0.008	-0.832	1.084
LJW.7	1.453	|	-0.219	0.017	0.023	-0.853	0.478	0.345	0.961	1.445
LJW.8	0.819	|	0.167	0.010	0.041	-0.546	0.196	0.445	0.524	0.430
LJW.9	6.112	|	1.021	0.365	0.028	4.521	13.412	0.547	3.411	18.220

	cos2	
LJW	0.008	|
LJW.1	0.197	|
LJW.2	0.303	|
LJW.3	0.313	|
LJW.4	0.019	|

```
LJW.5  0.502 |

LJW.6  0.857 |

LJW.7  0.437 |

LJW.8  0.410 |

LJW.9  0.311 |


Variables

         Dim.1    ctr    cos2    Dim.2    ctr    cos2    Dim.3    ctr    cos2

P2O5  |  0.646 13.594  0.418 |  0.600 21.968  0.360 |  0.160  3.721  0.026 |

TiO2  |  0.921 27.594  0.848 | -0.316  6.092  0.100 |  0.052  0.399  0.003 |

K2O   |  0.889 25.723  0.791 | -0.371  8.410  0.138 |  0.114  1.903  0.013 |

Fe2O3 |  0.886 25.565  0.786 | -0.180  1.986  0.033 | -0.015  0.035  0.000 |

Cu    |  0.449  6.564  0.202 |  0.555 18.818  0.308 | -0.690 69.388  0.476 |

S     |  0.172  0.960  0.029 |  0.837 42.727  0.700 |  0.411 24.554  0.169 |
```
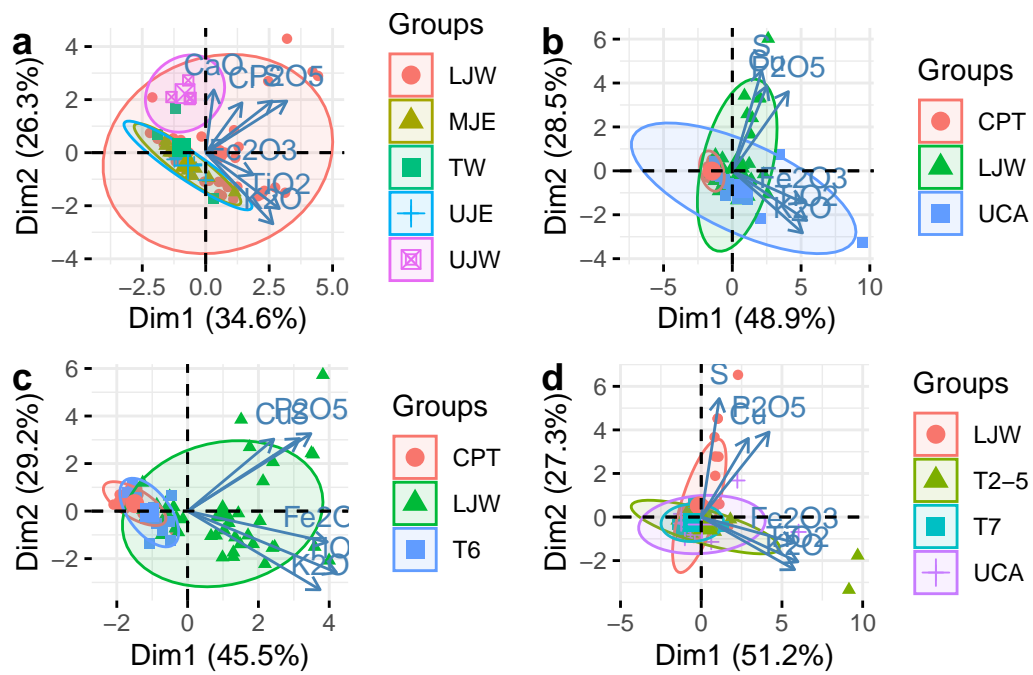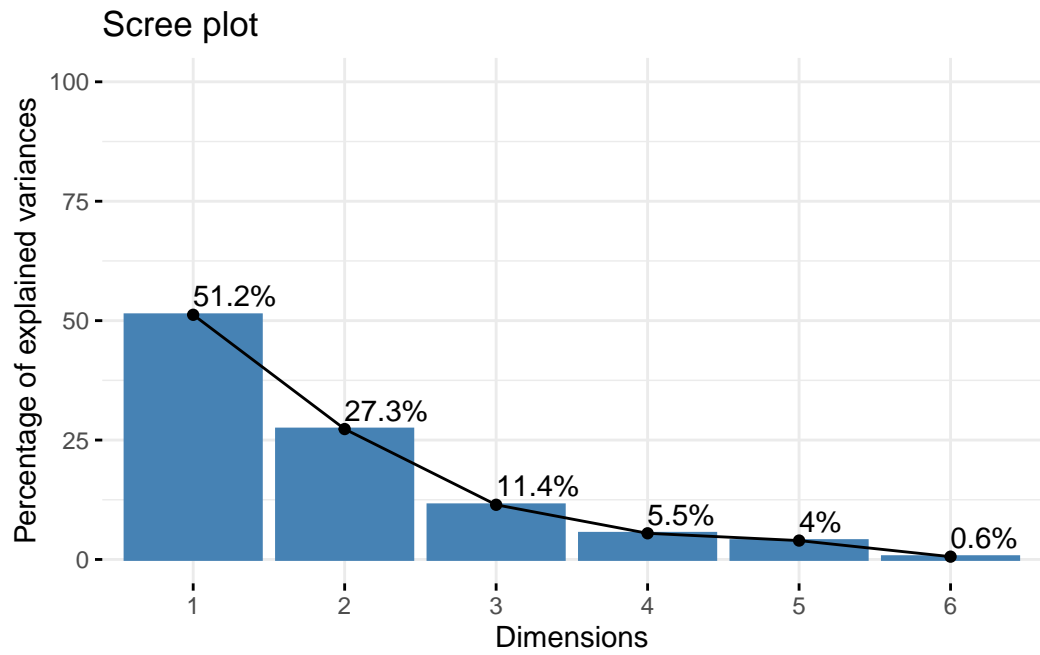
Figure 5.3: Several pcas

5.4 Methodology

For this experiment, a Bruker portable XRF Titan S1 was used in a laboratory benchtop setup, using battery power (up to 25% battery charge then replaced by a fully charged battery). A validation run was applied on two standard samples provided by Bruker and using the standard calibration. Samples were scanned for 180 seconds each (90 seconds for the first phase for major elements and 90 seconds for the second phase for minor elements), at least once, with several scans applied to samples that showed macroscopic variability (e.g., areas with different colours or translucency). The standard database from Bruker was used, with the Geochem application and Dual Mining method. ** chert samples were scanned, from several sources and chert types, both geological and archaeological. After scanning, the scanned face was measured (thickness and diameter), to guarantee a minimum thickness and size was followed for each sample, since other studies have shown thickness and size may impact the homogeneity of data collection and results (Newlander et al. 2015). All samples, including their thickness and diameter, can be found in table X. For geological samples, fresh, flat surfaces were scanned, avoiding altered faces or cortex; whenever necessary, the samples were prepared by breaking the nodules. The samples were chosen to represent all varieties of chert identified in the Algarve region, in the archaeological record of Vale Boi, but also from other regions such as Central Portugal and South Spain, to allow their comparison and test hypotheses made from macroscopic and petrographic data. For archaeological samples, artefacts were chosen from previously identified types (REF?), focusing on larger and flatter morphologies, with the least degree of surface alterations possible.

The analysis and result reporting protocol was established following previous studies, focusing on the accuracy of obtained data but also the transparency and reproducibility of

the results (Newlander et al. 2015; Johnson et al. 2024). For further reproducibility and replicability, and working towards the goal of open science (Johnson et al. 2024; Marwick 2017), the obtained raw pXRF results can be found online on our online compendium (LINK).

5.5 Results

The pXRF measured several major and minor elements, of which a small amount returned values of 0 or were below the limit of detection (<LOD). These were uranium (U), thorium (Th), bismuth (Bi), thallium (Tl), mercury (Hg), platinum (Pt), tantalum (Ta), hafnium (Hf), lanthanum (La), antimony (Sb), Tin (Sn), cadmium (Cd), rhodium (Rh), niobium (Nb), selenium (Se), zinc (Zn), nickel (Ni), cobalt (Co) and chromium (Cr). They were removed from the analysis based on their nonexistence, although they can still be found in the raw pXRF results.

6 From Stone to Tool

7 Discussion and final remarks

References

Johnson, Kimberly, Colin P. Quinn, Nathan Goodale, and Richard Conrey. 2024. "Best Practices for Publishing pXRF Analyses." *Advances in Archaeological Practice* 12 (2): 156–62. https://doi.org/10.1017/aap.2024.6.

Knuth, Donald E. 1984. "Literate Programming." *Comput. J.* 27 (2): 97–111. https://doi.org/10.1093/comjnl/27.2.97.

Marwick, Ben. 2017. "Computational Reproducibility in Archaeological Research: Basic Principles and a Case Study of Their Implementation." *Journal of Archaeological Method and Theory* 24 (2): 424–50. https://doi.org/10.1007/s10816-015-9272-9.

Newlander, Khori, Nathan Goodale, George T. Jones, and David G. Bailey. 2015. "Empirical Study of the Effect of Count Time on the Precision and Accuracy of pXRF Data." *Journal of Archaeological Science: Reports* 3 (September): 534–48. https://doi.org/10.1016/j.jasrep.2015.07.007.

Johnson, Kimberly, Colin P. Quinn, Nathan Goodale, and Richard Conrey. 2024. "Best Practices for Publishing pXRF Analyses." *Advances in Archaeological Practice* 12 (2): 156–62. https://doi.org/10.1017/aap.2024.6.

Knuth, Donald E. 1984. "Literate Programming." *Comput. J.* 27 (2): 97–111. https://doi.org/10.1093/comjnl/27.2.97.

Marwick, Ben. 2017. "Computational Reproducibility in Archaeological Research: Basic Principles and a Case Study of Their Implementation." *Journal of Archaeological Method and Theory* 24 (2): 424–50. https://doi.org/10.1007/s10816-015-9272-9.

Newlander, Khori, Nathan Goodale, George T. Jones, and David G. Bailey. 2015. "Empirical Study of the Effect of Count Time on the Precision and Accuracy of pXRF Data." *Journal of Archaeological Science: Reports* 3 (September): 534–48. https://doi.org/10.1016/j.jasrep.2015.07.007.

A Supplementary materials 1

Some supplementary materials.